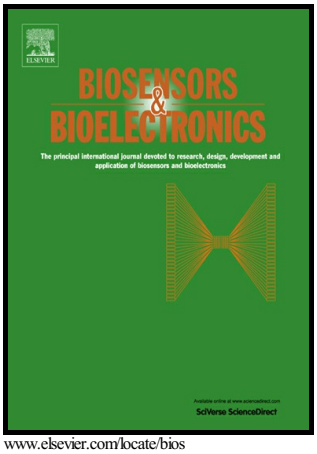

www.elsevier.com/locate/bios

Label-free piezoelectric biosensor for prognosis and diagnosis of Systemic Lupus Erythematosus

Noelle M. do Nascimento, Augusto Juste-Dolz, Elena Grau-García, Jose A. Román-Ivorra, Rosa Puchades, Angel Maquieira, Sergi Morais, David Gimenez-Romero

PII: S0956-5663(16)31142-3
DOI: http://dx.doi.org/10.1016/j.bios.2016.11.004
Reference: BIOS9323

To appear in: *Biosensors and Bioelectronic*

Received date: 9 September 2016
Revised date: 29 October 2016
Accepted date: 2 November 2016

Cite this article as: Noelle M. do Nascimento, Augusto Juste-Dolz, Elena Grau García, Jose A. Román-Ivorra, Rosa Puchades, Angel Maquieira, Sergi Morais and David Gimenez-Romero, Label-free piezoelectric biosensor for prognosis and diagnosis of Systemic Lupus Erythematosus, *Biosensors and Bioelectronic* http://dx.doi.org/10.1016/j.bios.2016.11.004

Label-free piezoelectric biosensor for prognosis and diagnosis of Systemic Lupus Erythematosus

Noelle M. do Nascimento[1], Augusto Juste-Dolz[2], Elena Grau-García[3], Jose A. Román-Ivorra[3], Rosa Puchades[1], Angel Maquieira[1], Sergi Morais[1*], David Gimenez-Romero[2*]

[1]Instituto Interuniversitario de Investigación de Reconocimiento Molecular y Desarrollo Tecnológico (IDM-Departamento de Química), Universitat Politècnica de València, Camino de Vera s/n, 46022 Valencia, Spain

[2]Departamento de Química-Física, Universitat de València, C/ Dr. Moliner 50, 46100 Burjassot, Spain

[3]Servicio de Reumatología, Hospital Universitario y Politécnico La Fe, Avenida de Fernando Abril Martorell nº 106, 46026 Valencia, Spain

smorais@qim.upv.es

David.Gimenez–Romero@uv.es

[*]Corresponding author.

ABSTRACT

An autoantigen piezoelectric sensor to quantify specific circulating autoantibodies in human serum is developed. The sensor consisted on a quartz crystal microbalance with dissipation monitoring (QCM-D) where TRIM21 and TROVE2 autoantigens were covalently immobilized, allowing the selective determination of autoantibodies for diagnosis and prognosis of Systemic Lupus Erythematosus (SLE). The sensitivity of the biosensor, measured as IC_{50} value, was 1.51 U/mL and 0.32 U/mL, for anti-TRIM21 and anti-TROVE2 circulating autoantibodies, respectively. The sensor is also able to establish a structural interaction fingerprint pattern or profile of circulating autoantibodies, what allows scoring accurately SLE patients. Furthermore, a statistical association of global disease activity with TRIM21-TROVE2 interaction was found (n = 130 lupic patient samples, p-value = 0.0413). The performances of the biosensor were compared with standard ELISA and multiplex DVD-array high-throughput screening assays, corroborating the viability of piezoelectric biosensor

as a cost-effective in vitro assay for the early detection, monitoring or treatment of rare diseases.

Keywords

Systemic Lupus Erythematosus, diagnosis, interaction fingerprint, immunosensor, quartz crystal microbalance, dissipation monitoring

1. INTRODUCTION

Systemic lupus erythematosus is a chronic inflammatory autoimmune disease (Chan et al., 2012) that adversely affects nearly every organ (skin, heart, lungs and intestines) of the human body, what makes it a harmful and high morbi-mortality illness (http://www.lupus.org/). SLE is generally considered the model systemic autoimmune disease, affecting 40-50 people per 100,000 with a 9:1 female-to-male ratio (WHO, 2006). Furthermore, both the genetic and non-genetic components of ethnicity influence in the expression and outcome of SLE.

The symptoms developed by SLE patients vary considerably from person to person and are quite similar to other common rare diseases what make the diagnosis of lupus difficult (Buhl et al., 2009). Therefore, the Systemic Lupus Collaborating Clinics (SLICC) employs stringent methodology requirements as criteria for SLE classification. As far as the diagnosis of SLE is concerned, the patient must satisfy at least 4 out of 17 SLICC requirements, including at least one clinical and one immunological criterion.

One of the main disadvantages of the clinical practice to diagnose SLE is that many indexes are subjective, because the scoring relies on reporting the symptoms by the patients rather than objective documentation and quantitative analytical results. This makes difficult to differentiate patients with multiple mild manifestations from those with severe symptoms. As no single criterion can describe the status for all the SLE patients, a Systemic Lupus Erythematosus Disease Activity Index (SLEDAI) is also used for diagnosis. The index is used by the physician to evaluate the patient records and as a measure of global disease activity in the clinic. The interpretation of the index has been shown to be reliable and valid. However, SLEDAI is focused on new or recurrent manifestations and fails to capture on-going activity.

According to several studies, the determination of specific autoantibodies facilitates the diagnosis of lupus (Rubin et al., 2014). These autoantibodies have been a cornerstone in understanding pathogenesis, supporting the management and treatment of SLE (Rubin and Konstantinov, 2016). Autoantibodies are typically present many years before the diagnosis of the disease and their presence tends to follow a predictable course, with a progressive accumulation before the onset of SLE, while patients are still asymptomatic (Eriksson et al., 2011).

Patients with autoimmune rheumatic diseases, such as SLE, have multitude of circulating autoantibodies against intracellular autoantigens (Biesen et al., 2016; Fritsch et al., 2006; Hu, et al., 2014; Defendenti et al., 2011). The primary autoantigens are U1-ribonucleoproteins, Sm, topoisomerase I, Jo-1, and Ro52/TRIM21, Ro60/TROVE2, and La (Fritsch et al., 2006). However, not all of the autoantibodies are specific for a particular autoantigen but they are useful biomarkers to help ruling in or out systemic autoimmune rheumatic diseases. Among the most common autoantibodies are those that target the autoantigens TRIM21 and TROVE2 (Al kindi et al., 2016).

The measurements to diagnose SLE consider the concentration of anti-Ro/SSA autoantibodies against the entire Ro complex, but few bioassays tests are capable to determinate the concentration of the specific autoantibodies to their two main components (TRIM21 and TROVE2). In fact, both autoantigens are major targets of the immune system in patients suffering with SLE and they are determined during the course of organ-specific autoimmune diseases. Therefore, the clinical prognostic and therapeutic utility of determining anti-TRIM21/TROVE2 circulating autoantibodies is of great interest (Menendez et al., 2013).

Regarding the quantitative methods for diagnosis, several assays have been developed for the determination of autoantibodies including, ELISA, line blot immunoassays, multiplex flow immunoassay and protein arrays (Infantino et al., 2013). Key advantages of these assays are its ease of use, flexibility, and low cost. However, the main limitation is concerned with the low sensitivity what limits the determination of the extremely low concentrations of circulating antibodies in serum. Therefore, the development of high sensitive biosensors is of great interest to determine autoantibodies at very low concentrations.

Quartz Crystal Microbalance (QCM) technique has been used extensively in biosensing (Cheng et al., 2011), because its good performance such as accuracy, stable oscillators and capability for label-free detecting subnanogram mass changes in real-time. It shows high

temperature dependence and lack multiplexing and high-throughput capabilities. (Pesquero et al., 2010). Nevertheless, the high sensitivity and low detection limits of QCM sensors offer excellent advantages over traditional sensing techniques. In particular, QCM-D (Quartz Crystal Microbalances with Dissipation) displays unique properties of sensing mass as well as viscoelastic effects together in single set of measurements (more than 200 data points per second), giving an innovative perspective in the domain of sensitivity range. In addition, QCM-D is attractive due to sensor response in the form of variations in the dissipation factor (ΔD) that is related to the viscoelasticity, which in turn is often associated to structural changes of the film adhering on the QCM-D transducer. This adds complementary information in relation with structural interactions between probe and target. In this sense, Hussain *et al.* (2016) reported the good performances of QCM-D, beating the standard coagulometer in terms of sensitivity range and information for hemostasis of human plasma.

The main goal of this research is therefore to develop high sensitive QCM-D based label-free biosensors for monitoring anti-TRIM21 and anti-TROVE2 circulating autoantibodies in a dynamic context. This would allow setting a characteristic interaction fingerprint pattern as consequence of the associated structural changes of the film during the molecular autoantigen-autoantibody recognition event. To the best of our knowledge, there are no reports of biosensing anti-TRIM21 and anti-TROVE2 circulating autoantibodies in human serum at low concentrations to diagnose and predict SLE disease. The new biosensing approach was used to test a pool of positive and negative sera, establishing a specific interaction pattern for SLE patients and healthy subjects. Furthermore, the performance of label-free biosensor was compared with the results displayed by standard ELISA plate and multiplex DVD-array high-throughput screening assays, showing the high potential of the QCM-D biosensing approach to diagnose and predict SLE.

2. MATERIALS AND METHODS

2.1. Patients and Samples

A total of 145 SLE patients and 8 healthy individuals provided full-informed written consent for this observational study. The approvals were obtained from the Biomedical Research Ethics Committee of the University and Polytechnic La Fe Hospital (Valencia, Spain). All patients agreed to take part in the study and satisfy the SLICC-ACR2012 classification criteria (Petri et al., 2012). The patients underwent complete medical

examination upon enrolment, and in the clinical visit lupus disease activity was assessed using the SLE Disease Activity Index (SLEDAI) (Gladman et al., 1992). Blood samples were collected by venipuncture of forearm veins from patients and healthy controls. Blood was collected in Vacutainer tubes containing EDTA, centrifuged for 15 minutes at 1,500 rpm, aliquoted (0.5 mL) into cryo tubes, and immediately frozen at -80 °C in La Fe Biobank. The samples were managed by the La Fe Biobank, PT13/0010/0026, following the criteria and ethical and legal requirements established by the 14/2007 Biomedical Research Law and 1716/2011 Royal Decree of Biobank Activity Rules.

A pool of fifty anti–Ro+ SLE patients' sera (SLE IgG) was purified by affinity chromatography (GE Healthcare, HiTrapTM protein G HP). The purified IgGs were used as autoantibodies standards. In the same manner, a pool of eight healthy subjects' sera (healthy IgG) was purified by affinity chromatography. The concentration of anti-TRIM21 and anti-TROVE2 autoantibodies of each patient was quantified by means of a human anti-SSA(Ro-52) ELISA kit and a IgG anti-SSA 60 kDa ELISA kit (Dia Pro Diagnostic Bioprobes), respectively. The optical density of each well was measured using a microplate reader (Wallac, Victor 1420 multilabel counter) at 450 nm.

The screening assay was performed on a regular DVD. Briefly, the polycarbonate surface of the DVD was coated with the autoantigens (TRIM21 and TROVE2) in microarray format (see supplementary material). The samples (sera) was directly dispensed onto the array (25 µL) and incubated at 37 ºC for 15 min. Then, the disc was washed with PBST and rinsed with deionized water. The immunoreaction was detected and amplified using anti-human IgGs labelled with gold and the silver enhancement solutions, respectively. A detailed description of the assay protocol is included in the supplementary material. The results of the DVD assays were analysed as previously described (Morais *et al*., 2010).

2.2. Quartz crystal microbalance with dissipation monitoring (QCM-D)

QCM-D measurements were carried out using commercially available gold Q-sense sensors (5 MHz, QSX 301, Biolin Scientific). The variation of frequency and dissipation was monitored using a Q-Sense E1 device equipped with a liquid flow cell setup. All experiments were carried out in 10 mM phosphate buffer saline (PBS), pH 7.4 at a flow rate of 50 µL/min at 25 °C.

The piezoelectric quartz crystal chip was first cleaned by UV irradiation (254 nm) for 10 min. Then, the chip was immersed in a solution of 5:1:1 of milli-Q water, ammonia 25% and H_2O_2 30% at 75 °C for 5 min. Next, the chip was rinsed with milli-Q water, and blown dry with nitrogen. Finally, the chip was treated with UV again during 10 min. Self-assembled monolayer (SAM) was performed by immersing the quartz crystal in 10 mM MPA solution (3-mercaptopropionic acid) overnight and then activated with 46 mM of EDC -N-ethyl-N'-(3-dimethylaminopropyl) carbodiimide, NHS (N-hydroxysuccinimide) 98% for 1 h.

After activation of SAM, the chip was treated with 5 mM carbohydrazide 98 % for 1 h. Next, 100 µL of the buffered autoantigen solution (33 mg/L of TRIM21 (recombinant human RO-52/SS-A expressed in E. Coli, Sigma-Aldrich) or TROVE2 (recombinant human RO-60/SS-A expressed in E. Coli, long isoform, ProSpec) was dispensed over the sensor and incubated for 1 hat room temperature. The crosslinked residues were blocked by immersing the god sensor in a 1 M ethanolamine-HCl ≥ 98% solution for 1 h and next, in a blocking buffer solution, containing 1 mM ethylenediaminetetraacetic acid (Riser), 0.25% bovine serum albumin (BSA, Sigma-Aldrich, ≥98% agarose gel electrophoresis), and 0.05% Tween-20 (Scharlau, synthesis grade) (Hong et al., 2009). Next, the chip was rinsed with milli-Q water and blown dry with nitrogen. The sensing chips were characterized by Static Water Contact Angle (SCA), Polarization Modulation Infrared Reflection Absorption Spectroscopy (PM-IRRAS) and X-ray Photoelectron Spectroscopy (XPS), as described in Supplementary Material.

The sensing chip was placed into the flow module with the side coated with the autoantigen facing up. The system temperature was adjusted to 25 °C at a flow rate of 50 µL/min. Then, PBS was circulated on the surface sensor until stabilization. The resonance frequency was monitored until a steady baseline was obtained (f_0). Then, 1.0 mL of autoantibodies standards at different concentrations (0.02-3.0 U/mL for anti-TRIM21 and 0.01-1.5 U/mL for anti-TROVE2) were recirculated into the system for 1 h to reach the steady state. Next, PBS buffer was injected into the flow to remove bulk effects on viscoelastic properties of sensor chip. When the resonance frequency reached a stable value, another steady state resonant frequency was taken (f_1). The frequency shifts ($\Delta f = f_0 – f_1$) induced by the protein-autoantibody binding was the difference between the value displayed before reaction (f_0) and the final value (f_1). The frequency shifts were correlated precisely to the change of surface concentration using the Sauerbrey equation (17.7/n ng cm^{-2} Hz^{-1}, n is the harmonic number). The mean value was the average of two replicates. The dose-curve

was plotted according to the relationship between surface concentrations and autoantibody concentrations. BSA and active human crystallisable region (Fc, Abcam, active human IgG FC fragment) were used as negative controls.

The biosensor was regenerated, accomplishing a desorption step, using 0.1 M glycine/HCl, pH 2.5 at a flow rate of 50 µL/min at 25 °C.

2.3. Statistical method

Data are presented as the mean (standard deviation) and median (1st, 3rd quartile) in the case of continuous variables and as relative and absolute frequencies in the case of categorical variables. Differences in continuous variables among groups were assessed using Wilcoxon rank-sum test. Relationships among different variables were evaluated using linear regression, ordinal regression and logistic regression as appropriate. Differences were considered significant at p-values less than 0.05. All statistical analyses and graphs were performed using the R software (The R Project for Statistical Computing, https://www.r-project.org/).

3. RESULTS

3.1. QCM-D-based TRIM21 biosensor

Although both TRIM21 and TROVE2 take part in the Ro/SSA RNP complex, the expression level of the TRIM21 protein is higher than that of TROVE2. For this reason, the QCM-D-based biosensor was optimized first for the detection of circulating autoantibodies to TRIM21 antigen. In this study, a direct immunoassay was developed where the simple binding between the TRIM21 antigen and its respective autoantibody was label-free detected by the QCM-D biosensor. The sensing surface consisted in gold-coated QCM-D quartz crystals with TRIM21 covalently immobilized via a SAM. As Figure 1a shows, recombinant human TRIM21 protein was immobilized onto the gold chip using 3-mercaptopropionic acid as a monolayer precursor and subsequent covalent EDC coupling (surface concentration 267 ng/cm^2, coverage percentage close to 100%).

The immobilization process of TRIM21 and TROVE2 on the gold surface was characterized by XPS, PM-IRRAS, DPI and SCA (Figure 1). After the addition of MPA acid (Figure 1b), the sulphur percentage measured by XPS increased (0-4.69%), also increasing

the SCA (56.9º-69.01º). The EDC/NHS reaction and the addition of carbohydrazide induced an increase of the nitrogen percentage (0-3.53%), decreasing consequently the SCA (69.01º-55.8º). Finally, the immobilization of the TRIM21 protein and the blockage process rendered a clear increase of carbon (55.60-63.70%) and nitrogen (3.53-12.30%) percentages, as expected after these immobilisation steps. The SCA remained virtually constant (55.80º-56.70º).

PM–IRRAS spectra of the fabricated SAM was performed in the 4,000-800 cm^{-1} spectral range (Figure 1c). The spectral bands revealed the presence of proteins, and the homogeneity and high-structural order in the gold surface was demonstrated by the high-defined peaks. Finally, the C-terminal-oriented immobilization of TRIM21 was monitored by DPI (Figure 1d). The protein orientation depends on the surface coverage. First, the protein was anchored in a vertical orientation (thickness/molecule about 14 nm/molecule). However, as the surface coverage increases, DPI monitored a restructuring of the monolayer, in which the TRIM21 molecule orientation changed from a vertical (14 nm/molecule) towards a flat-on manner orientation (6 nm/molecule). The TRIM21 theoretical dimensions confirm the process of the protein deposition, about 21.4×7.4×5.6 nm. Hence, the surface characterization corroborated the formation of a hydrophilic SAM of TRIM21 with high structural order and surface homogeneity.

The piezoelectric biosensor operates on the principle that a change in mass, resulting from the interaction between the autoantibody (biomarker) and its respective autoantigen (immobilized probe), can be directly determined (Figure 2a). The dependence of the apparent mass change on the bulk concentration of anti-TRIM21 autoantibody standards from SLE patients (0.02-3.0 U/mL, see Materials and Methods section) was stablished. As Figure 2b shows, the surface concentration of the antigenic complex increases as the bulk concentration of SLE IgG standards increases. The signals were fitted to the general Hill equation (R^2=0.99) (Figure 2b). Using this fitting, the calculated limit of detection (LOD) of the assay for anti-TRIM21 autoantibodies was 0.01 U/mL. This LOD was established according to the concentration given by the interpolation of the blank signal (0 ng/cm^2) plus 3 times the standard deviation (SD, 8.85 ng/cm^2). The limit of quantification (LOQ), calculated as the concentration given by the interpolation of the blank signal plus ten times the SD of the blank measurements, was 0.04 U/mL. The assay sensitivity calculated from the half-maximal inhibitory concentration (IC_{50}), was 1.51 U/mL, with a dynamic range (DR, defined presenting the transition from 20% to 80% maximal signal) between 0.32 and 7.17 U/mL.

The reproducibility of the measurements was within the range 5 to 10%. Herein, it is important to emphasize that the developed biosensor is able to determine TRIM21 within a low concentration range, discriminating well the negative control (BSA, signal equal to zero). In comparison to the ELISA plate format (IC_{50} 117 U/mL and LOD 1.2 U/mL), the developed QCM-D biosensor was 120 times more sensitive and alleviated the need for labelled secondary antibodies as well.

In order to discriminate between SLE and healthy subjects, the recognition event which involves only the antibody standards from healthy donors was also studied (Figure 2b). As in the previous study, the evolution of the surface concentration of the antigenic complex was studied according to the bulk concentration of healthy IgG standards (control IgGs). The obtained response was also evaluated via the general Hill equation (R^2= 0.95). However, a substantial change in the antibody selectivity is observed, depending on the standard origin, which shows that anti-TRIM21 autoantibodies from patients and healthy subjects have different affinity (maximum surface concentration 766 ng/cm^2 for SLE standard and 110 ng/cm^2 for healthy standard).

The reason why the developed QCM-D-based TRIM21 biosensor showed non-zero signal for health subjects (Figure 2c) is probably due to the capability of the PRY-SPRY domain to recognize Fc (McEwan et al., 2013). The cut-off for scoring patients with SLE was stablished at 110 ng cm^{-2}, corresponding to a concentration of TRIM21 of 0.2 U/mL.

The accuracy of the analytical methods generally decreases by the presence of different circulating endogenous factors. A commonly used strategy to remove or decrease the matrix effect is the sample dilution, which works well with immunoassays exhibiting very high sensitivity (Ramakrishna and Mehan, 1993). Thus, a fit-for-purpose assessment was performed for the analysis of serum samples in order to demonstrate the applicability of the piezoimmunosensor in the clinical practice. Figure 2c shows how the signal due to non-specific interactions of the matrix (sera pool without immunoglobulins G) of SLE patients (yellow bars) and healthy subjects (blue bars) decreases as the serum is diluted. The matrix effect of the QCM-D-based TRIM21 biosensor is below the cut-off value for 1:100 diluted serum samples (80 ng cm^{-2} from SLE patients and 107 ng cm^{-2} from healthy subjects).

3.2. QCM-D-based TROVE2 biosensor

Both TRIM21 and TROVE2 proteins are part of the Ro/SSA RNP complex, so the determination of the concentration of anti-TROVE2 autoantibodies is also of great interest. Recombinant human TROVE2 protein was immobilized onto a gold QCM-D sensor via 3-mercaptopropionic acid as a monolayer precursor and covalent EDC/NHS coupling (surface concentration 194 ng/cm^2, coverage percentage 91%). As for TRIM21, the immobilization process was characterized systematically with XPS, SCA and DPI measurements. As is shown in Figure 1, the immobilization of TROVE2 was correctly completed. The immobilization step induced a clear increase of the carbon (11.1%-53.8%) and nitrogen (0%-9.3%) percentage, whereas the SCA remained virtually constant (56.9º-56.7º) as is depicted in Figure 1b.

C-terminal-oriented immobilization of TROVE2 was monitored by DPI. Figure 1e shows how the protein orientation depends on the surface coverage. Firstly, the protein is deposited in a vertical orientation (thickness/molecule = 9 nm/molecule). However, as surface coverage increases and therefore, steric effects are higher, DPI monitors a change in the TROVE2 immobilization from a vertical orientation towards a flat-on manner, 9 to 3 nm/molecule. The measured TROVE2 dimensions are 8.5×5.5×3 nm (Stein et al., 2005). Therefore, theoretical data confirm the proposed orientation. As in the previous case, we generate a hydrophilic SAM with high structural order and surface homogeneity.

Figure 2b shows how the surface concentration of the antigenic complex detected by the developed piezoimmunosensor increases as the concentration of SLE IgG standard also upturns (0.01-1.5 U/mL). This progression can be described using the general Hill equation (R^2=0.99), reaching a LOD of 0.005 U/mL. This LOD is 400 times more sensitive than the commercial ELISA test (LOD 2.0 U/mL). On the other hand, the LOQ was 0.019 U/mL and the IC_{50} 0.32 U/mL, with a DR from 0.07 to 1.46 U/mL. The negative binding control gave early zero signal for all the range of concentrations employed, corroborating the selectivity of the biosensor and the absence of unspecific interactions. In contrast to the case of TRIM21, the response of the developed biosensor for TROVE2 is only due to epitope-paratope specific interactions since the piezoelectric signal was zero when active human antibody Fc fragment was used as negative binding control.

In order to discriminate between SLE and healthy subjects (Figure 2b) the recognition involving healthy IgG standards was also studied. The obtained piezoelectric response was

adjusted with a nonlinear Hill model (R^2 = 0.99), showing a substantial change in the autoantibody affinity (maximum surface concentration 440 ng/cm^2 for SLE IgG standards and 150 ng/cm^2 for healthy IgG standards). The anti-TROVE2 autoantibodies have different paratopes depending on the standard origin. Hence, the established cut-off value for this biosensor was 150 ng/cm^2 (110 ng/cm^2 for the QCM-D-based TRIM21 biosensor). This value allows identifying easily between a pathologic (> 0.16 U/mL) and normal status (< 0.16 U/mL). In order to unify sensing criteria, the cut-off value for TRIM21 and TROVE2 piezoimmunosensors should be set at 150 ng/cm^2.

Figure 2c shows how the piezoelectric signal due to non-specific interactions of the matrix (sera pool without immunoglobulins G) of SLE patients (black bars) and healthy subjects (brown bars) decreases as the dilution of the serum increased. In both cases, the matrix effect was removed by diluting the serum 100 times (5.9 ng/cm^2). Hence, the developed QCM-D-based TROVE2 biosensor determine the concentration of anti-TROVE2 autoantibodies in a 1:100 serum dilution. In conclusion, TRIM21 and TROVE2 piezoimmunosensors quantify with good sensitivity anti-TRIM21 and anti-TROVE2 autoantibodies in human serum in a label-free way without previous purification steps.

Reusability is one of the main issues found in biosensing. To estimate the piezoimmunosensor mean life, repeated analyses of anti-TRIM21 standards (1.5 U/mL) were carried out. After the regeneration step, the sensor chip was considered useful while the piezoelectric signal remained above 90% of the initial value. In a continuous work, the piezo signal remained constant for at least 30 assay cycles. More than 30 assay cycles resulted in a significant loss of the piezo signal. Therefore, the useful life of the sensor was established as 30 assay cycles. Considering the mean life of the piezoimmunosensors, the tiny amount of immobilized target required, and the non-need of using auxiliary immunoreagents for detection, a price of 2€ per assay is estimated. However, the price can be significantly reduced when the sensors were manufactured in mass.

3.3. Interaction fingerprint pattern

The main advantage of QCM-D compared with the conventional QCM, is the possibility of measuring both changes in resonant frequency (f) and, the energy loss or dissipation (D) of the system. In this manner, both signals were measured and the $-\partial f/\partial D$ function was calculated, providing the reaction path of the monitored interaction. This path is specific of

the studied biochemical system, which could allow SLE patients and healthy subjects to be scored. In this way, the developed piezoimmunosensors can simultaneously determine circulating autoantibodies concentration working as a traditional sensor and additionally given information about the interaction fingerprint pattern that is related with the structural interaction profile.

As is depicted in Figure 2, the autoantibodies from patients and control subjects have a different recognition mechanism of the recombinant human TRIM21. In view of that, using the developed biosensor, the interaction fingerprint pattern was established from the $-\partial f/\partial D$ function. For that, 80,000 data points with three coordinates (time, f, D) was measured at real time for each biomarker concentration (0.06-8.0 U/mL) during 3,000 s. Figure 3 shows how the TRIM21-IgG reaction path is different for SLE patients and healthy subjects. Thus, in SLE patients, the $-\partial f/\partial D$ function is a peak-shape function whose peak intensity does not depend on the bulk concentration of anti-TRIM21 autoantibodies, 19 Hz at 1,000 s. However, the $-\partial f/\partial D$ function from healthy subjects has the same characteristics than from SLE IgGs, but with a constant peak intensity about 9 Hz at 600 s (8.8 Hz at 1,000 s), which is 2.1 times lower than in the patient group. Consequently, an interaction fingerprint pattern was established for the fast identification of anti-TRIM21 circulating autoantibodies from SLE patients in human serum samples. This pattern represents the structural interaction profile of the sick antigenic complex and could be a selection criterion for further screening strategies. Moreover, it can be applied to detect false positive ($-\partial f/\partial D < 10$ Hz at 1,000 s) and to improve the true positive rate ($-\partial f/\partial D = 19$ Hz at 1,000 s) of the developed ultrasensitive immunosensor. The $-\partial f/\partial D$ function allows taking advantage of the huge information offered by the protein conformational dynamics.

Following this step, the TROVE2-antibody interaction fingerprint pattern was also calculated. Figure 3 shows how this pattern is not such a specific pattern of SLE. The reaction path of this interaction was found to be similar for SLE patients and control subjects, and independent on the bulk concentration of anti-TROVE2 standards (0.2-27 U/mL). It is a peak-shape function with a maximum value of 11 Hz at 1,000 and of 9 Hz at 300 s (8.6 Hz at 1,000 s) for autoantibodies from SLE patients and healthy subjects, respectively. Both values are very similar and consequently, it is not possible to differentiate easily between SLE patients and healthy subjects through this pattern. The only feasible pattern for characterizing the SLE patient group is the TRIM21-antibody interaction fingerprint.

3.4. Biostatistics

As Hanly et al. reported (2010), there is a significant association between elevated global SLE disease activity index SLEDAI (which is a tool used to quantify the symptoms of patients with SLE) and the concentration of anti-Ro circulating autoantibodies. Consequently, an ordinal regression model (n = 130 real samples from SLE patients) was used to evaluate the association of global SLE disease activity with the concentration of anti-TRIM21 and anti-TROVE2 and the interaction between both.

No statistical association of activity index with the anti-TRIM21 and anti-TROVE2 concentration was found (p-value = 0.335 and 0.109, respectively). However, there was a statistical effect considering the TRIM21-TROVE2 interaction (p-value = 0.0413). Thus, the simultaneous measurement of both autoantibodies may become an important part of the overall assessment of SLE patients in clinical practice. For the characterization of SLE patients, it is very important to determine simultaneously the individual concentration of anti-TRIM21 and anti-TROVE2 autoantibodies in serum (quantification of the symptoms of patients with SLE), as well as to establish an interaction fingerprint pattern (SLE diagnosis). .

3.5. Screening assay

A duplex immunoassay would have the ability to detect both biomarkers (anti-TRIM21 and anti-TROVE2) concurrently in a single biological sample, along with negative and positive binding controls. As a first approximation, a microarray detection system based on the compact disc technology (Morais et al., 2010) was used. A non-competitive sandwich immunoassay for the simultaneous determination of circulating anti-TRIM21 and anti-TROVE2 immunoglobulins was employed, as a proof of concept (Figure 4a).

Under the optimized conditions (see Supplementary Material), the sensitivity of the assays, measured as IC_{50}, the limit of detection (LOD), and dynamic range were determined. The calibration curves obtained for the simultaneous determination of the multiplexed immunoassays are shown in Figure 4b. The standard curve for the anti-TRIM21 biomarker was fitted using the four-parameter Gompertz equation (R^2 = 0.997), because the diffusion of reactants greatly influence the assay response at these experimental conditions (Avella-Oliver et al., 2013), reaching a LOD, of 11 U/mL and a IC_{50} value of 96 U/mL. On the other hand, for the anti-TROVE2 biomarker, the calibration curve was fitted from the four-parameters Hill equation (R^2 = 0.995), reaching a of LOD of 58 U/mL and a IC_{50} of 228 U/mL. Herein,

it is important to emphasize that cross-reactivity was not detected at these experimental conditions. The relative standard deviation values along the whole calibration curve were below 10%. It is also worth mentioning that multiplexed immunoassay reached similar sensitivity (IC_{50}) of ELISA plate format (IC_{50} 117 and 42 U/mL for anti-TRIM21 and antiTROVE2 in ELISA assay, respectively), and it was much less sensitive than QCM-D-based label-free biosensor (IC_{50} 1.51 and 0.32 U/mL for anti-TRIM21 and antiTROVE2 in ELISA assay, respectively).

4. CONCLUSION

The main advantage of using QCM-D biosensors for Systemic Lupus Erythematosus diagnosis is three fold. First, the ultra-sensitive biosensing approach allows the determination of circulating anti-TRIM21 and anti-TROVE2 autoantibodies in human serum at low U/mL levels. In comparison to current used analytical methodologies, the sensitivity reached by QCM-D biosensors is two orders of magnitude higher than ELISA tests, offering the possibility to detect the disease much earlier than the symptoms arise, since autoantibodies are typically present many years before the diagnosis of SLE, while patients are still asymptomatic. Secondly, using a novel $-\partial f/\partial D$ function the QCM-D-based biosensor provided accurate real time information about molecular interaction fingerprint pattern or profile. This complementary information could be used in the clinical practice to characterize subjects with systemic autoimmune disease, providing the specific fingerprint of the TRIM21-autoantibody binding pattern.

The analysis of the data of 130 patients gave statistical association of global SLE disease activity with the TRIM21-TROVE2 interaction. Consequently, the full characterization of the SLE patient group might be done by measuring simultaneously the TRIM21-antibody binding fingerprint pattern and the concentration of circulating anti-TRIM21 and anti-TROVE2 autoantibodies. Indeed, the developed biosensors allow the simultaneous diagnosis (TRIM21-antibody binding fingerprint pattern) and prognosis (determination of anti-TRIM21 and anti-TROVE2 autoantibodies) of SLE patients. The measurement of both circulating autoantibodies may become an important part of the overall management and treatment of SLE. Third, the QCM-D biosensors allow for a label free detection of circulating autoantibodies molecules, offering new insights in the molecular recognition process by exploring the kinetics and thermodynamics of specific interactions.

The developed immunoassay on a regular DVD could be implemented into the accelerated monitoring protocols due to the multiplex capability and the good sensitivity. However, the main disadvantage compared to the QCM-D sensor is that it does not give additional information that facilitates the full characterization of SLE patients.

To our knowledge, the QCM-D technology is an interesting sensing approach to characterize SLE patients. Indeed, the developed piezoimmunosensors may be a cornerstone in long-term studies to monitor the stability of anti-TRIM21 and anti-TROVE2 autoantibody profiles over time, predicting clinical events and examining the significance of a change in concentration of circulating autoantibodies.

The ideal biosensor for SLE diagnostic applications should be label-free, multiplex, sensitive, allowing the direct measurement of the structural interaction profile. The multichannel quartz crystal microbalance array with dissipation monitoring might be a good option that could meet the requirements to implement a biosensing tool in the routine clinical practice for the early detection, monitoring or management of rare diseases.

DECLARATION OF INTEREST

The authors declare no competing financial interests.

ACKNOWLEDGEMENTS

We acknowledge financial support from the Generalitat Valenciana (GVA–PROMETEOII/2014/040) as well as the Spanish Ministry of Economy and Competitiveness and the European Regional Development Fund under award numbers CTQ2013–45875–R and CTQ2013–42914–R.

REFERENCES

Al Kindi, M.A., Colella, A.D., Chataway, T.K., Jackson, M.W., Wang, J.J., Gordon, T.P., 2016. Autoimmun Rev. 15, 405-401.

Avella-Oliver, M., Gimenez-Romero, D., Morais, S., González-Martínez, M.A., Bueno, P.R., Puchades, R., Maquieira, A., 2013. Chem. Commun. 49, 10868-10870.

Biesen, R., Rose, T., Hoyer, B.F., Alexander, T., Hiepe, F., 2016. Lupus 25, 823-829.

Buhl, A., Page, S., Heegaard, N.H., von Landenberg, P., Luppa, P.B., 2009. Biosens. Bioelectron. 25, 198-203.

Chan, V.S., Nie, Y.J., Shen, N., Yan, S., Mok, M.Y., Lau, C.S., 2012. Autoimmun Rev. 11, 890-897.

Cheng, C.I., Chang, Y.P., Chu, Y.H. 2012. Chem. Soc. Rev. 41, 1947-1971.

Defendenti, C., Atzeni, F., Spina, M.F., Grosso, S., Cereda, A., Guercilena, G., Bollani, S., Saibeni, S., Puttini, P.S., 2011. Autoim. Rev. 10, 150-154.

Eriksson, C., Kokkonen, H., Johansson, M., Hallmans, G., Wadell, G, Rantapää-Dahlqvist, S., 2011. Arthritis Res. Ther. 13, R30.

Fritsch, C., Hoebeke, J., Dali, H., Ricchiuti, V., Isenberg, D.A., Meyer, O., Muller, S., 2006. Arts. Reum. Ther. 8, R4.

Gladman, D., Ginzler, E., Goldsmith, C., Fortin, P., Liang, M., Urowitz, M., Bacon, P., Bombardieri, S., Hanly, J., Hay, E., Isenberg, D., Jones, J., Nived, O., Petri, M., Richter, M., Sanchez-Guerrero, J., Snaith, M., Sturfelt, G., Symmons, D., 1992. J. Rheumatol. 19, 1820-1821.

Hanly, J.G., Su, L., Farewell, V., Fritzler, M.J., 2010. J. Immunol. Methods 358, 75-80.

Hong, S.R., Choi, S. J., Jeong, H.D., Hong, S., 2009. Biosens. Bioelectron. 24, 1635-1640.

Hu, Z.D., Deng, A.M., 2014. Clin. Chim. Acta 437, 14-18.

Hussain, M., Northoff, H., Frank K Gehring, F.K., 2015. Biosens. Bioelectron, 66, 579-584.

Infantino, M., Bentow, C., Seaman, A., Benucci, M., Atzeni, F., Sarzi-Puttini, P., Olivito, B., Meacci, F., Manfredi, M., Mahler, M., 2013. Clin. Dev. Immunol. 2013, 978202.

McEwan, W.A., Tam, J.C.H., Watkinson, R.E., Bidgood, S.R., Mallery, D.L., James, L.C., 2013. Nat. Immunol. 14, 327–336.

Menendez, A., Gomez, J., Escanlar, E., Caminal-Montero, L., Mozo, L., 2013. Autoimmunity, 46, 32-39.

Morais, S., Tamarit, J., Puchades, R., Maquieira, A., 2010. Environ. Sci. Technol. 44, 9024-9029.

Pesquero, N.C., Pedroso, M.M., Watanabe, A.M., Goldman, M.H., Faria, R.C., Roque-Barreira, M.C., Bueno, P.R., 2010. Biosens. Bioelectron. 26, 36-42.

Petri, M., Orbai, A.M., Alarcón, G.S., Gordon, C., Merrill, J.T., Fortin, P.R., et al. 2012. Arthritis Rheum. 64, 2677-2686.

Ramakrishna, N., Mehan, V.K., 1993. Mycotoxin. Res. 9, 53-63.

Rubin, R.L., Wall, D., Konstantinov, K.N., 2014. Biosens. Bioelectron. 51, 177-83.

Rubin, L.R, Konstantinov, K.N., 2016. Biosens. Bioelectron. 83, 306-311.

Stein, A.J., Fuchs, G., Fu, C., Wolin, S.L., Reinisch, K.M., 2005. Cell 121, 529-537.

World Health Organization, 2006. Environmental Health Criteria 236, WHO Press, Geneva.

Yoo, G., Bong, J.H., Kim, S., Jose, J., Pyun, J.C., 2014 Biosens. Bioelectron. 57, 213-218.

LEGEND OF THE FIGURES

Figure 1.- Surface characterization of the QCM-D-based Ro biosensors: a) Scheme of the immobilization of the autoantigens TRIM21 and TROVE2. b) Atomic percentage measured by XPS, and SCA, during the protein immobilization process. c) PM–IRRAS spectra of the Ro SAM in the 4000–800 cm^{-1} spectral range. d) Thickness per molecule measured by DPI during the oriented immobilization of TROVE2 and e) TRIM21.

Figure 2.- a) Measurement scheme of the developed piezoimmunosensor. The blue and red lines correspond to the frequency and dissipation factor changes monitored during the antigen-antibody recognition, respectively. b) Calibration curves for anti-TRIM21α and anti-TROVE2 autoantibodies from SLE patients and healthy subjects. c) Effect of serum matrix on the analytical signal of the developed QCM-D sensor .

Figure 3.- Interaction fingerprint pattern for the TRIM21α -autoantibody binding obtained using sera of SLE patients and healthy subjects.

Figure 4.- a) Scheme of the microarray detection system on a standard DVD. b) Calibration curves for anti-TRIM21α and anti-TROVE2 circulating autoantibodies.

Highlights

An ultrasensitive superantigen piezoelectric sensor to determine circulating autoantibodies for SLE diagnosis and prognosis is developed.

The sensor establishes an interaction fingerprint pattern of circulating autoantibodies, distinguishing clearly SLE patients from healthy donors.

A statistical association of global disease activity with TRIM21-TROVE2 interaction was found (n = 130 lupic patient samples, p-value = 0.0413).

a)

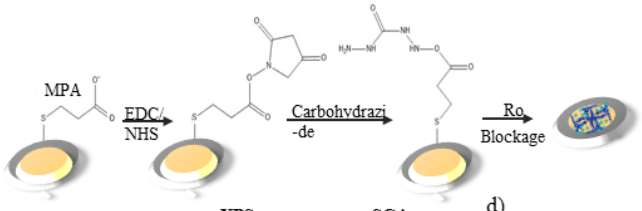

b)

	XPS					SCA
QCM-D Chip	% Au	% C	% O	% S	% N	Degree (°)
Cleaned	84.81	11.10	4.09	-----	-----	56.9
MPA	38.17	41.26	15.87	4.69	-----	69.01
EDC/NHS	19.29	52.35	23.14	2.06	3.23	59
Carbohydrazide	26.24	55.60	11.99	2.63	3.53	55.8
Ro	29.9	46.6	10.9	3.3	9.3	-----
Ro/blockage	19.3	53.8	12.2	2.3	12.4	56.7

c)

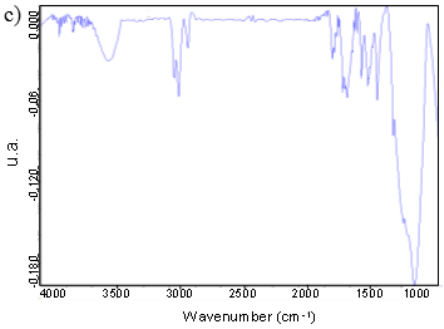

d)

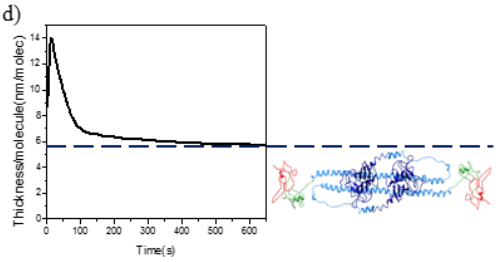

e)

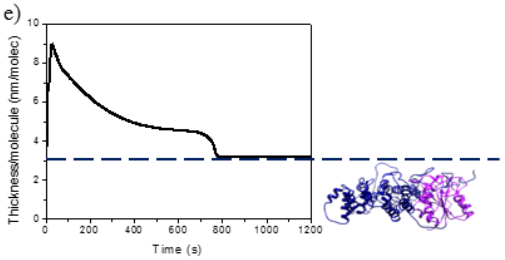

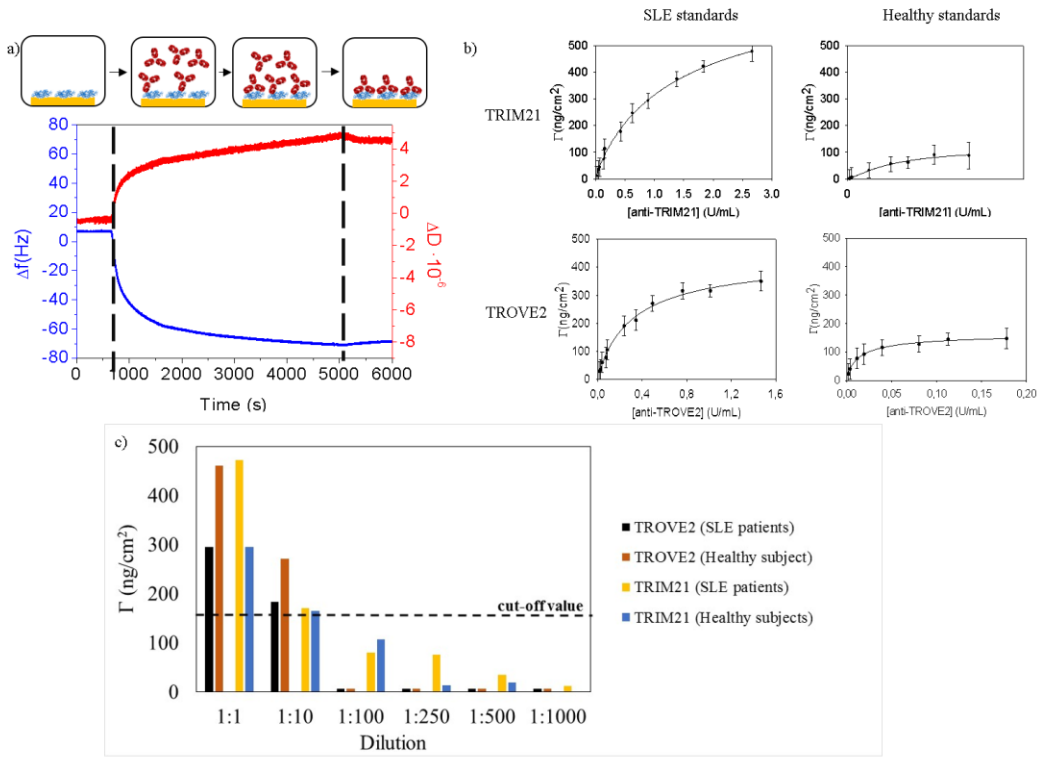
a)
Δf(Hz)
ΔD ·10⁻⁶
Time (s)
b)
SLE standards
Healthy standards
TRIM21
TROVE2
Γ(ng/cm²)
[anti-TRIM21] (U/mL)
[anti-TROVE2] (U/mL)
c)
Γ (ng/cm²)
cut-off value
1:1
1:10
1:100
1:250
1:500
1:1000
Dilution
TROVE2 (SLE patients)
TROVE2 (Healthy subject)
TRIM21 (SLE patients)
TRIM21 (Healthy subjects)

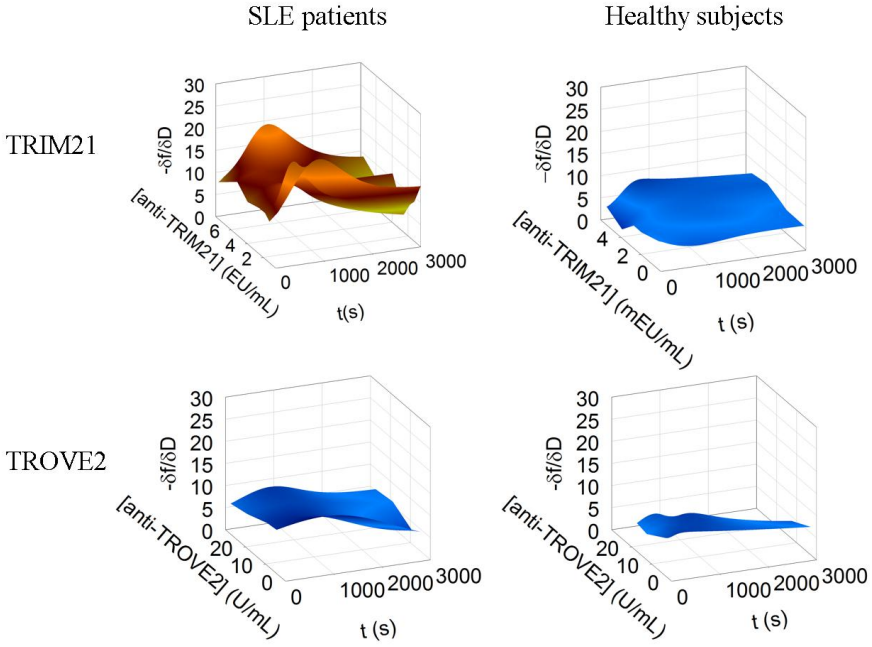
SLE patients
Healthy subjects
TRIM21
TROVE2
-δf/δD
[anti-TRIM21] (EU/mL)
[anti-TRIM21] (mEU/mL)
[anti-TROVE2] (U/mL)
t(s)
t (s)

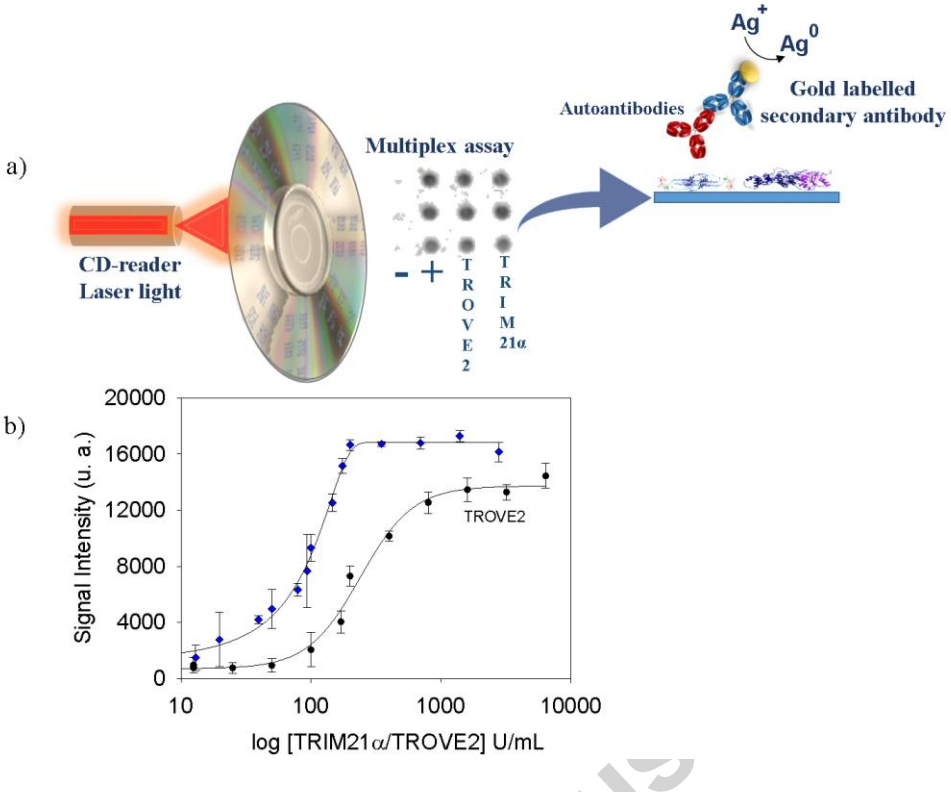
a)
Ag+
Ag0
Gold labelled
secondary antibody
Autoantibodies
Multiplex assay
CD-reader
Laser light
- +
TROVE2
TRIM21α
b)
Signal Intensity (u. a.)
20000
16000
12000
8000
4000
0
10
100
1000
10000
TROVE2
log [TRIM21α/TROVE2] U/mL

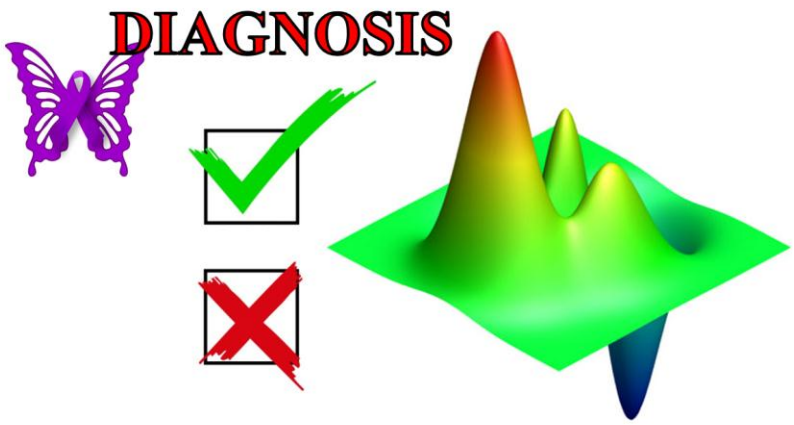
DIAGNOSIS